

## KCNE5 Induces Time- and Voltage-Dependent Modulation of the KCNQ1 Current

Kamilla Angelo, Thomas Jespersen, Morten Grunnet, Morten Schak Nielsen, Dan A. Klaerke, and Søren-Peter Olesen

Department of Medical Physiology, University of Copenhagen, The Panum Institute, Copenhagen, Denmark

**ABSTRACT** The function of the KCNE5 (KCNE1-like) protein has not previously been described. Here we show that KCNE5 induces both a time- and voltage-dependent modulation of the KCNQ1 current. Interaction of the KCNQ1 channel with KCNE5 shifted the voltage activation curve of KCNQ1 by more than 140 mV in the positive direction. The activation threshold of the KCNQ1+KCNE5 complex was +40 mV and the midpoint of activation was +116 mV. The KCNQ1+KCNE5 current activated slowly and deactivated rapidly as compared to the KCNQ1+KCNE1 at 22°C; however, at physiological temperature, the activation time constant of the KCNQ1+KCNE5 current decreased fivefold, thus exceeding the activation rate of the KCNQ1+KCNE1 current. The KCNE5 subunit is specific for the KCNQ1 channel, as none of other members of the KCNQ-family or the human *ether a-go-go* related channel (hERG1) was affected by KCNE5. Four residues in the transmembrane domain of the KCNE5 protein were found to be important for the control of the voltage-dependent activation of the KCNQ1 current. We speculate that since KCNE5 is expressed in cardiac tissue it may here along with the KCNE1  $\beta$ -subunit regulate KCNQ1 channels. It is possible that KCNE5 shapes the  $I_{Ks}$  current in certain parts of the mammalian heart.

### INTRODUCTION

It has become clear that channels are composed of numerous units, which engage into larger complexes. Often the pore-forming  $\alpha$ -subunits interact with other membrane proteins and/or couple to cytosolic components that contribute to the features of the channel. Some accessory proteins change the sensitivity of the  $\alpha$ -subunit to e.g.,  $Ca^{2+}$ , pH, temperature, cell volume changes, or second messengers. They may direct the membrane localization of channels, couple channels to the cytoskeleton, or regulate the expression level of channels. Basic channel properties such as selectivity, conductance, voltage-dependency and pharmacological profile can be changed by these subunit-interactions to an extent where the biophysical characteristics of the  $\alpha$ -subunit become difficult to recognize. Several important native currents have been proven to be composed of such subunits interacting in a non-trivial fashion (Seino, 1999; Peleg et al., 2002).

The KCNE-family is a group of small proteins, which interact with voltage-gated potassium channels. The length of the KCNE proteins is between 130 and 167 amino acids and they contain one transmembrane domain flanked by an extracellular N-terminal and a cytosolic C-terminal. The first member of the family, KCNE1 (minK), was cloned in 1988 (Takumi et al., 1988) and in 1999, Abbott et al. isolated KCNE2, 3 and 4 (MiRP1–3) (Abbott et al., 1999). The functional effect of KCNE1 on

the KCNQ1 channel is that the current activates and deactivates slower than when the KCNQ1  $\alpha$ -subunit is alone. The voltage sensitivity of the KCNQ1+KCNE1 current is shifted toward positive potentials and the whole-cell current density is increased. Furthermore, assembly of KCNQ1 with the KCNE1 subunit increases the unitary conductance by fourfold (Sesti and Goldstein, 1998). The current formed by the KCNQ1+KCNE1 complex corresponds to the slow delayed rectifier current,  $I_{Ks}$ , in cardiac myocytes (Sanguinetti et al., 1996; Barhanin et al., 1996). An interaction between KCNE3 and KCNQ1 gives rise to a constitutively open potassium channel that plays a role in cyclic AMP-stimulated  $Cl^-$  secretion (Schroeder et al., 2000; Grahammer et al., 2001). Expression of KCNQ1 together with KCNE2 in COS cells results in an effect similar to that of the KCNE3; the KCNQ1 channel transforms into a voltage-independent channel (Tinel et al., 2000a).

In 1999 Piccini et al. isolated a gene, which they refer to as the KCNE1-like gene. The KCNE1-like gene is one of the four genes that are deleted in the AMME contiguous gene syndrome (Jonsson et al., 1998). The human KCNE1-like protein shows 56% homology with KCNE1. It is composed of 142 amino acids and like the other members of the KCNE-family it has a single putative transmembrane domain. The KCNE1-like gene has lately been suggested to be the fifth member of the KCNE family and is now referred to as KCNE5 (Abbott et al., 2001). To date the function of the KCNE5 protein has not been established. Here we demonstrate that the KCNQ1 current is markedly influenced by the presence of KCNE5. We show that the KCNE5  $\beta$ -subunit affects the activation kinetics of the KCNQ1 current in the same direction as observed for the KCNE1+KCNQ1 complex;

Submitted March 12, 2002, and accepted for publication May 30, 2002.

Address reprint requests to Kamilla Angelo, Dept. of Medical Physiology, University of Copenhagen, The Panum Inst, Blegdamsvej 3, Copenhagen 2200 N, Denmark. Tel.: 45 35327445; Fax: 45 35327555; E-mail: angelo@mfi.ku.dk.

© 2002 by the Biophysical Society

0006-3495/02/10/1997/10 \$2.00

however, to a much greater extent. The voltage-activation curve of the KCNQ1 current is shifted in the positive direction toward an activation threshold of +40 mV. Thus, the KCNQ1+KCNE5 complex only conducts current upon strong and continued depolarization. The effect of KCNE5 was specific for KCNQ1 channels; the other KCNQ channels or the human *ether a-go-go* related channel (hERG1) was not affected by coexpressed KCNE5. Mutagenesis experiments showed that four specific amino acids in the transmembrane domain of KCNE5 are responsible for the regulatory effect.

## MATERIALS AND METHODS

### Molecular and cell biology

hKCNE5, obtained from IMAGE Consortium (EST AI086317, ID 1655937) was PCR amplified and inserted into a custom-made vector (pXOOM) optimized for expression in both *Xenopus laevis* oocytes and mammalian cells (Jespersen et al., 2002). Similarly the hKCNQ1-5, hERG1 and hKCNE1 were inserted in pXOOM. The pXOOM construct includes the sequence of the enhanced green fluorescent protein (EGFP), which was used as a marker of successfully transfected cells. The E5/E1 chimera was generated by an overlap extension procedure where the four KCNE1-encoding codons were introduced by oligonucleotides. The integrity of all constructs was confirmed by sequencing.

CHO-K1 cells were cultured according to instructions by American Type Culture Collection (Manassas, VA). Transfections were done according to the manufacturer's instructions with Lipofectamine and Plus reagent in Optimem1 (GibcoBRL, Life Technologies, Rockville, MD). Cotransfections of  $\alpha$ - and  $\beta$ -subunits were made in a 1:1 molar ratio of the cDNA.

### Electrophysiology

Recordings were made using an EPC9 patch-clamp amplifier controlled by HEKA pulse software version 8.30 (HEKA Electronics, Lambrecht, Germany). Input data were Bessel-filtered at 1.7 kHz and sampled at 5 kHz. All experiments were performed in the whole-cell configuration with borosilicate glass pipettes pulled to a resistance of 1.5–3 M $\Omega$ . The series resistance was always below 10 M $\Omega$  and was 80% compensated. Capacitive transients were automatically cancelled during an experiment (Sigworth et al., 1995). No leak subtraction was done. *Xenopus* oocyte recordings were performed as previously described (Grunnet et al., 2001).

The standard extracellular solution contains (in mM): 140 NaCl, 4 KCl, 1 MgCl<sub>2</sub>, 2 CaCl<sub>2</sub>, and 10 Hepes titrated with NaOH to pH 7.4. The standard intracellular solution contains (in mM): 110 KCl, 5.2 CaCl<sub>2</sub>, 1.4 MgCl<sub>2</sub>, 10/30 EGTA/KOH, and 10 Hepes titrated with KOH to pH 7.2. The liquid junction potential of the standard solution was calculated to 6.8 mV; however, this was not corrected for in the presented data with the exception of the reversal potentials of Fig. 4 B. During experiments the extracellular solution was flowing at a rate of 0.5–1 ml/min and the cell chamber volume was 20  $\mu$ l. The temperature of the bath solution was controlled by an inline heater (Warner Instruments, Hamden, CT). XE991 was provided by NeuroSearch A/S, Denmark. A stock of 100 mM was prepared in DMSO and diluted in extracellular solution before use.

### Data analysis

Fitting procedures and other data analysis were done using the IGOR software version 4.04 (Wavemetrics, Lake Oswego, Oregon). To calculate

values of  $V_{1/2}$  the peak amplitudes of tail currents were fitted to the Boltzmann equation:

$$I_{\text{tail}}(V_m) = I_{\text{min}} + \frac{I_{\text{max}} - I_{\text{min}}}{1 + \exp \times ((V_{1/2} - V_m)/\text{slope})}$$

where  $V_{1/2}$  is the potential of half-maximal activation and the slope is  $kT/ze$ . To determine time constants of activation the current traces from channel activation were fitted to the single-exponential equation:

$$I(t) = A \times (1 - \exp(-t/\tau_{\text{act}}))$$

where  $\tau_{\text{act}}$  is the time constant of activation and  $A$  is the current amplitude at infinite time. To determine time constants of deactivation tail current traces were fitted to the double-exponential equation:

$$I(t) = (A_{\text{fast}} \times \exp(-t/\tau_1)) + (A_{\text{slow}} \times \exp(-t/\tau_2))$$

where  $A_{\text{fast}}$  and  $A_{\text{slow}}$  are current amplitudes at time 0.  $\tau_1$  and  $\tau_2$  are the time constants of the fast and slow components, respectively.

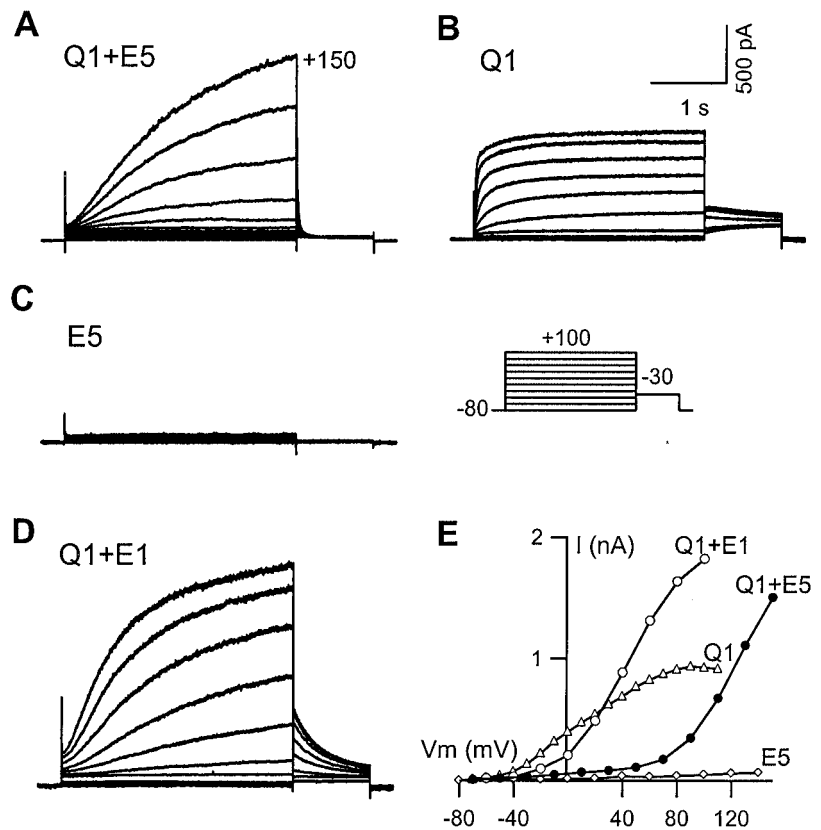
The average is presented as mean  $\pm$  S.E. Student's  $t$ -tests were performed using Microsoft Excel. Statistical significance was taken at  $p < 0.05$ .

## RESULTS

### Characteristics of the KCNQ1+KCNE5 current

To test if the KCNE5 (E5) protein interacts with KCNQ1 (Q1) the subunits were coexpressed in CHO cells and the electrical properties of the cells were studied by the patch-clamp technique. Fig. 1 illustrates currents recorded from whole-cell experiments performed in physiological solutions on transiently transfected CHO cells. The cells were clamped at a holding potential of  $-80$  mV and stimulated for 3 s at potentials from  $-80$  to  $+100$  or  $+150$  mV in intervals of 5 s. Every depolarization was followed by a step to  $-30$  mV for 1 s (see Protocol). The Q1+E5 current is illustrated in Fig. 1 A. In presence of the E5 subunit both the kinetics and the voltage sensitivity of the KCNQ1 channel changed significantly as compared to Q1 alone (Fig. 1 B). The Q1+E5 current required long and strong depolarization to activate. The activation threshold of the Q1+E5 current was  $+40$  mV and activation was still incomplete after 3 s of depolarization (Fig. 1 A). When the Q1  $\alpha$ -subunit was expressed alone it activated at voltage-depolarizations above  $-50$  mV and in contrast to the Q1+E5 current, the Q1 current was fully activated within 500 ms. Expression of KCNE5 alone did not yield any current (Fig. 1 C). This indicates that the current recorded from Q1+E5-transfected cells is not derived from channels formed solely by E5 proteins or by E5 and endogenous channels in the CHO cell. Currents recorded from a cell cotransfected with the KCNQ1 channel and the KCNE1 (E1) subunit are illustrated in Fig. 1 D. The Q1+E1 complex activated slower than the Q1 current, however still faster than the Q1+E5. The activation threshold for the Q1+E1 was  $-20$  mV, which was a right-shift compared to the activation thresh-

**FIGURE 1** Effect of KCNE5 on the KCNQ1 current. Representative whole-cell recordings from CHO cells transfected with Q1+E5 (A), Q1 (B), E5 (C), and Q1+E1 (D). Recordings were performed in standard physiological solutions and the cells were clamped at a holding potential of  $-80$  mV. Every 5 s the cells were stimulated with a 3-s pulse of voltages from  $-80$  to  $+100$  mV or  $+150$  mV in steps of  $10$  mV and tail currents were recorded by stepping to  $-30$  mV for 1 s. For clarity only every second trace is presented. The scale bar accounts for all traces. (E) The IV-relationship of the recordings in A–D. The current amplitudes were measured at the end of the 3-s pulse and plotted as a function of the potential.  $\Delta$ , Q1;  $\bullet$ , Q1+E5;  $\diamond$ , E5;  $\circ$ , Q1+E1.



old of Q1 current alone, but the change in voltage sensitivity was much smaller than for Q1+E5.

The current-voltage relationships of the recordings in Fig. 1, A–D, are presented in Fig. 1 E. The current densities measured at  $+100$  mV were  $21 \pm 5$  pA/pF ( $n = 7$ ) for Q1 alone,  $66 \pm 9$  pA/pF ( $n = 12$ ) for Q1+E1, and  $55 \pm 11$  pA/pF ( $n = 20$ ) for Q1+E5. Thus cotransfection of Q1 with E5 increased the current amplitude at  $+100$  mV by more than twofold as compared to Q1 alone.

The deactivation kinetics was another feature of the Q1 current that was significantly influenced by the E5 subunit. Within 50 ms the Q1+E5 current was deactivated by approximately 80% (higher resolution is shown in Fig. 5). In contrast, the tail of Q1+E1 (Fig. 1 D) did not reach zero during the  $-30$  mV pulse showing that the channels required more than 1 s to deactivate fully.

In Fig. 2 the peak amplitudes of normalized tail currents recorded at  $-30$  mV are plotted as a function of the prepulse potential for a representative experiment of Q1, Q1+E1 and Q1+E5, respectively. The midpoints of activation were calculated by fitting to the Boltzmann equation. The  $V_{1/2}$  value of Q1 alone was  $-24$  mV and when coexpressed with E1 it was  $+29$  mV. However, when Q1 and E5 were expressed together the  $V_{1/2}$  shifted in the positive direction by more than  $140$  mV. The  $V_{1/2}$  of the experiment presented in Fig. 2 was  $+116$  mV. The data behind this  $V_{1/2}$  value of Q1+E5 are from tail currents measured after

prepulses ranging from  $-80$  to  $+150$  mV. As can be seen from the fitted line the plateau of the activation curve for the Q1+E5 channels lay above  $+150$  mV, thus the  $V_{1/2}$  value should be considered an estimate.

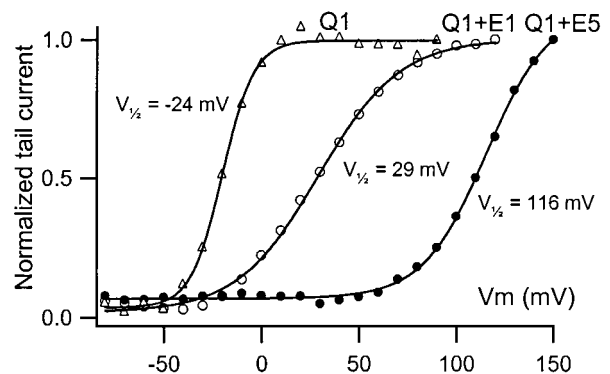


**FIGURE 2** The activation curve of the KCNQ1+KCNE5 current. Representative activation curves of Q1 ( $\Delta$ ), Q1+E1 ( $\circ$ ), and Q1+E5 ( $\bullet$ ). The peak of the tail currents measured at  $-30$  mV were normalized to the tail current determined by a preceding prepulse at  $80$  mV (for Q1),  $120$  mV (for Q1+E1), and  $150$  mV (for Q1+E5), respectively. Tail current data were fitted to the Boltzmann function and the midpoints of activation were calculated:  $V_{1/2}$  of Q1 alone =  $-24$  mV ( $-22 \pm 3$  mV,  $n = 4$ );  $V_{1/2}$  of Q1+E1 =  $29$  mV ( $36 \pm 6$  mV,  $n = 6$ ); and  $V_{1/2}$  of Q1+E5 =  $116$  mV ( $109 \pm 2$  mV,  $n = 5$ ).

To ensure that the Q1+E5 current was not a phenomenon specific to CHO cells we expressed Q1 and E5 in COS cells. We found no apparent difference between the two mammalian expression systems (data not shown).

Piccini et al. (1999) tested the potential function of E5 as a  $\beta$ -subunit for Q1 in *Xenopus* oocytes but found no effect of E5. We also investigated the possible interaction between the two proteins in the oocyte expression system. After injection of E5 RNA with or without Q1 RNA the resting potential of the oocytes, which is normally  $-50$  to  $-40$  mV gradually shifted in the positive direction to potentials of  $-10$  to  $0$  mV within 48 h. No Q1+E5 current or Q1 current were recorded in these oocytes. In experiments of delayed injection, where Q1 channels were expressed before the injection of E5 RNA, the Q1 current was suppressed within 16–18 h after E5 injection and the same shift in the resting potential was observed. This indicates that E5 inhibits the Q1 channels expressed in the oocytes; however, no Q1+E5 current was ever detected. The Q1+E5 current may be masked by large endogenous  $\text{Na}^+$  currents, which were induced by the prolonged voltage-depolarization (Baud et al., 1982).

### Block of KCNQ1+KCNE5 by XE991

The compound XE991, a derivative of linopiridine, is a marker of KCNQ currents (Robbins, 2001). To show that the current recorded from CHO cells transfected with Q1 and E5 is a Q1 specific current, we applied  $100 \mu\text{M}$  XE991 to the extracellular solution and observed a complete and irreversible block of the current. In Fig. 3 A current traces from recording before and after addition of  $1.5 \mu\text{M}$  XE991 are depicted. The Q1+E5 current was activated by stepping to  $+80$  mV for 3 s every 5 s. When XE991 was added to the bath the Q1+E5 current was partly and irreversibly blocked within 2 min (Fig. 3 B). A  $K_d$  value was determined to  $1.4 \pm 0.5 \mu\text{M}$  ( $n = 4$ ) by fitting to the time course of blockade according to Strøbæk et al. 2000 (Strobaek et al., 2000).

### Ion selectivity of KCNQ1+KCNE5

In Fig. 4 the ion selectivity of the Q1 pore was studied in the presence of E5. The recordings were performed on CHO cells cotransfected with Q1 and E5 using bath solutions with different potassium concentrations. The tail currents in the insert of Fig. 4 A were elicited by clamping the cell at  $+100$  mV for 3 s and subsequently stepping to potentials between  $-120$  and  $+40$  mV (see Protocol). Instantaneous current-voltage relations were derived by plotting the peak amplitudes of the tails as a function of the potential. The instantaneous IV curves in Fig. 4 A were recorded with 4, 40, and 150 mM extracellular  $\text{K}^+$  ions. As the extracellular  $\text{K}^+$  concentration increases the reversal potential ( $V_{\text{rev}}$ ) becomes more positive. In Fig. 4 B the  $V_{\text{rev}}$  values have been

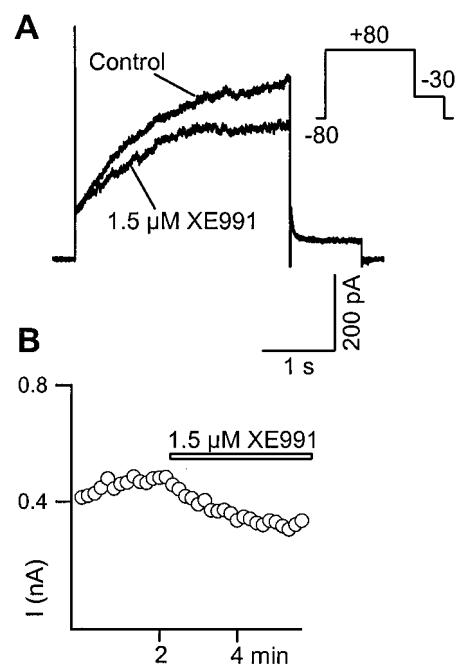
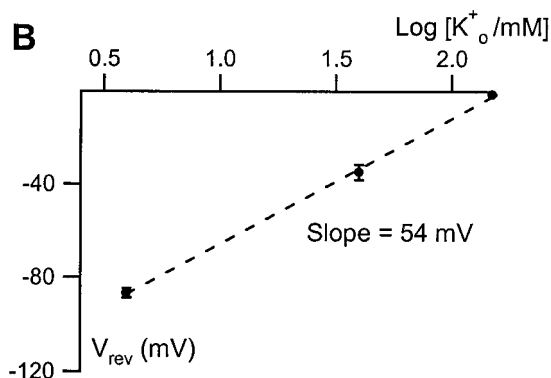
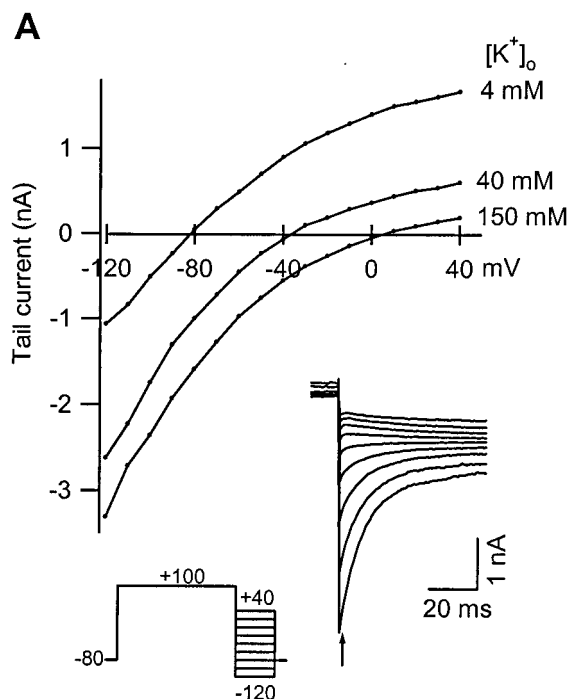


FIGURE 3 The KCNQ1+KCNE5 current was blocked by XE991. (A) A cell transfected with Q1 and E5 was pulsed every 5 s by clamping to  $+80$  mV for 3 s and to  $-30$  mV for 1 s (see Protocol). Current traces from recordings done before and after addition of  $1.5 \mu\text{M}$  XE991 to the bath are overlaid. (B) Time course of the experiment in A. The current was measured at the end of the 3-s pulse and plotted as a function of time. The Q1+E5 current was irreversibly blocked by XE991. A  $K_d$  value was determined to  $1.4 \pm 0.5 \mu\text{M}$  by fitting to the time course of blockade.

corrected for the liquid junction potential and plotted as a function of the logarithm of the extracellular potassium concentration. The slope of the straight line was 54 mV indicating high potassium selectivity; ideal potassium selectivity gives a slope of 59 mV.

### Time constants of activation and deactivation at 22°C and 37°C

The kinetics of the Q1+E5 and Q1+E1 currents are compared in Fig. 5. Representative currents of activation to  $+100$  mV and deactivation to  $-30$  mV have been normalized and superimposed. Subsequently the traces were fitted to an exponential function to determine the time constants. The activation traces were fitted to a single-exponential function, whereas the deactivation curves required a double-exponential function. Fig. 5 A and B show the results from recordings performed at room temperature ( $\sim 22^\circ\text{C}$ ) and Fig. 5 C and D show the results from recordings at  $37^\circ\text{C}$ . At  $22^\circ\text{C}$  the Q1+E5 current activated with a time constant of  $1251 \pm 90$  ms ( $n = 6$ ); in comparison, the Q1+E1 activated with a time constant of  $715 \pm 90$  ms ( $n = 3$ ). However, with a rise in temperature to  $37^\circ\text{C}$  the activation time constant of Q1+E5 dropped to  $262 \pm 34$  ms ( $n = 4$ ), whereas the



**FIGURE 4** Ion selectivity of the KCNQ1+KCNE5 complex. (A) Instantaneous current-voltage relations of the Q1+E5 current recorded in three different concentrations of extracellular potassium. The NaCl in the standard physiological solution was stoichiometrically substituted with KCl to final concentrations of 4, 40, or 150 mM extracellular potassium. The instantaneous IV relations were recorded by activating the channels for 3 s at +100 mV and subsequently stepping to potentials between -120 to 40 mV in increments of 10 mV (see Protocol). The insert shows tail currents recorded from a cell superfused with extracellular solution of 40 mM K<sup>+</sup> (for clarity only every second trace is presented). The current amplitudes measured at the peak of the tail (arrow) were plotted as a function of the potential from three representative experiments. The measured reversal potential ( $V_{rev}$ ) from recordings performed in  $[K^+]_o$  of 4 mM was  $-80 \pm 2$  mV ( $n = 4$ ); in  $[K^+]_o$  of 40 mM was  $-28 \pm 3$  mV ( $n = 3$ ); and in  $[K^+]_o$  of 150 mM was  $5 \pm 0$  mV ( $n = 3$ ). (B) The  $V_{rev}$  values, which have been corrected for the liquid junction potential are plotted as a function  $\log[K^+]_o$ . The slope of the straight line is 54 mV, indicative of strong K<sup>+</sup> selectivity.

Q1+E1 activation time constant only decreased to  $577 \pm 94$  ms ( $n = 3$ ). The differences in time of activation at both 22°C and 37°C are less pronounced at potentials below 100 mV.

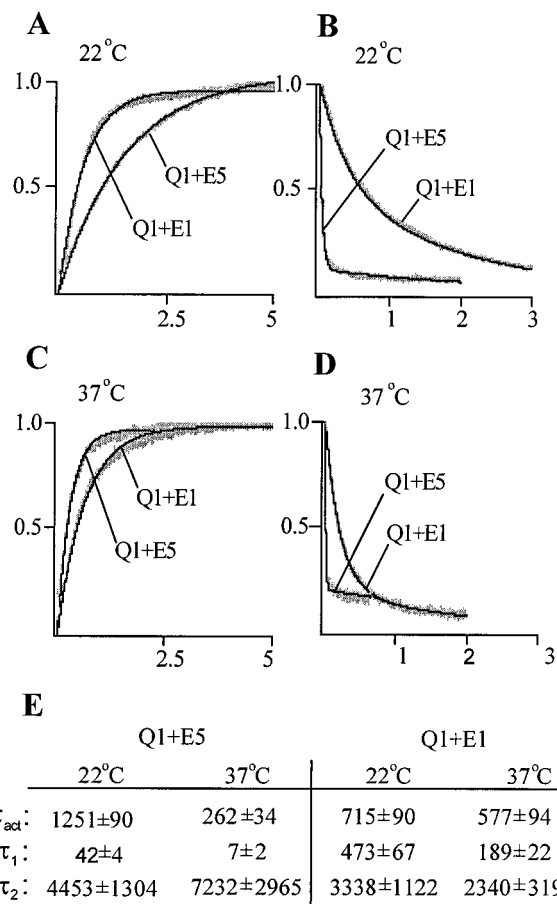


**FIGURE 5** Activation and deactivation kinetics of the KCNQ1+KCNE5 current, a comparison with the Q1+E1 current. Transfected CHO cells were depolarized to 100 mV for 5 s followed by a 2- to 3-s-long pulse to -30mV. Time constants were determined by fitting the activation traces to a single-exponential function and the deactivation traces to a double-exponential function. The illustrated traces have been normalized to the maximal current amplitude. Solid lines represent the fitted curves. (A) Superimposed traces from activation of Q1+E5 and Q1+E1 currents performed at 22°C. (B) Superimposed traces from deactivation of Q1+E5 and Q1+E1 currents performed at 22°C. (C) Superimposed traces from activation of Q1+E5 and Q1+E1 currents performed at 37°C. (D) Superimposed traces from deactivation of Q1+E5 and Q1+E1 currents performed at 37°C. (E) List of  $\tau$  values from exponential fitting. All values are in ms ( $n = 3-6$ ).

Under all conditions the Q1+E5 current deactivated fast compared to the Q1+E1 current. At 22°C the fast and slow deactivation constants of Q1+E5 were  $42 \pm 4$  ms and  $4453 \pm 1304$ , respectively. At 37°C the  $\tau$  values were  $7 \pm 2$  ms ( $\tau_1$ ) and  $7232 \pm 2965$  ms ( $\tau_2$ ). The fast components comprised a fraction of  $0.82 \pm 0.03$  and  $0.74 \pm 0.07$  of the total tail current amplitude at 22°C and 37°C, respectively. The slow component from the fitting to Q1+E5 tail currents can largely be attributed to leak. The Q1+E1 current deactivated with  $\tau_1$  values in the range of hundreds of ms at both 22°C and 37°C. The fraction of the fast components were  $0.60 \pm 0.07$  at 22°C and  $0.82 \pm 0.02$  at 37°C. All  $\tau$  value

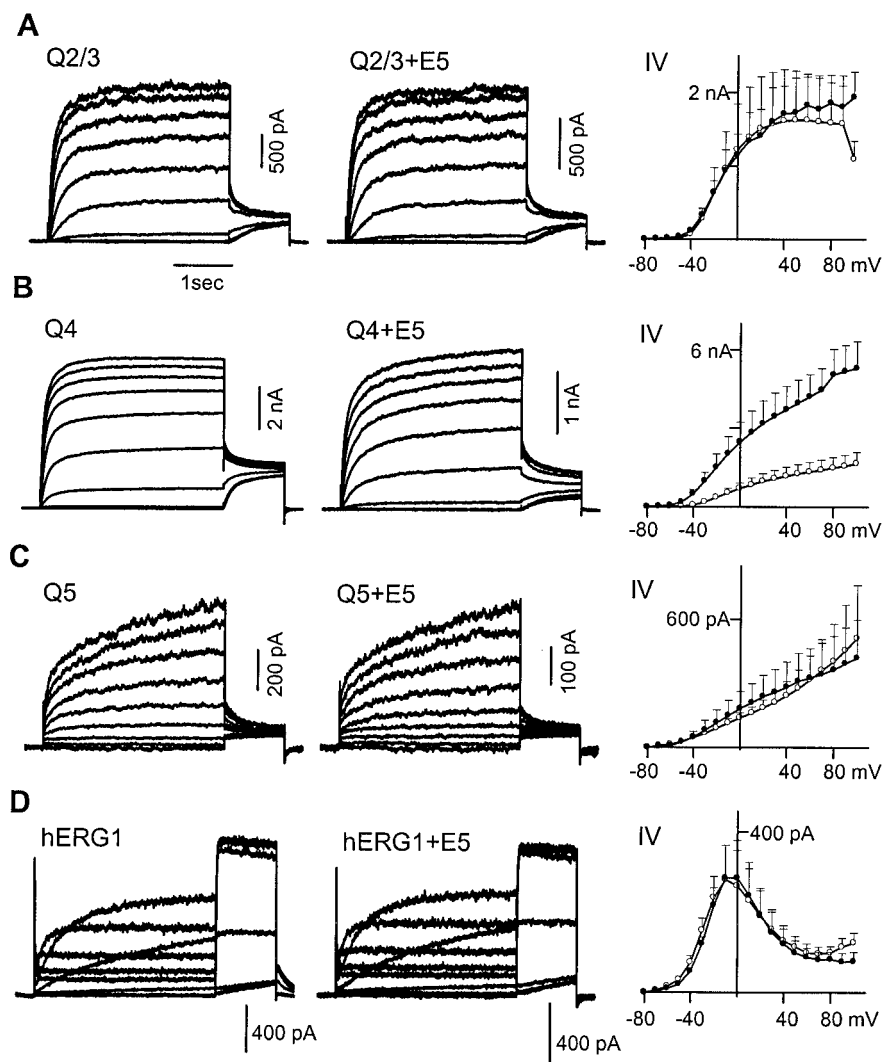


FIGURE 6 Specificity of KCNE5. Representative whole-cell currents recorded from CHO cells transfected with  $\alpha$ -subunit alone (left panel) and together with the E5 (center panel). (A) Q2/3, (B) Q4, (C) Q5, and (D) hERG1. The cells were voltage-clamped according to the protocol in Fig. 1. In the right panel the average current from between 4 and 10 experiments measured at the end of the depolarization pulse are plotted as a function of voltage. ●,  $\alpha$ -subunit alone; ○, with E5.

are listed in Fig. 5 E. The changes in temperature had no influence on the absolute voltage sensitivity of the channel complex; the activation threshold of Q1+E5 was still +40 mV at 37°C.

### Specificity of the KCNE5 $\beta$ -subunit

Some KCNE-subunits have the potential to interact with members of the KCNQ family other than the Q1 channel. KCNE2 modulates the deactivation kinetics of KCNQ2/3 (Q2/3) channels (Tinel et al., 2000b) and Schroeder et al. (2000) found that the KCNQ4 (Q4) current is inhibited in the presence of KCNE3 (Schroeder et al., 2000). As yet no  $\beta$ -subunit has proven to change the characteristics of the KCNQ5 (Q5) channel.

We have studied the possible effect of E5 on all known KCNQ channels. Each KCNQ  $\alpha$ -subunit was expressed in CHO cells with and without the E5 protein. Representative

whole-cell recordings of the Q2/3–5 channels alone and with E5 are illustrated in Fig. 6, A–C. The IV relations from 4–10 experiments are presented in the right panel. The current traces are scaled to the same size to allow direct comparison of the kinetics. No E5 effect was observed on the voltage sensitivity or the current kinetics for any of the Q2/3–5 channels.

In addition to the experiments performed on the KCNQ channel we tested for an E5-effect on the hERG1, which is the molecular component behind the rapid delayed rectifier current in cardiomyocytes ( $I_{Kr}$ ) (Abbott et al., 1999). The finding that E5 is expressed in the heart together with the negative result of a Q1+E5 interaction in oocytes lead Piccini et al. to speculate that the hERG1 channel may be a partner of the E5 protein. HERG1 is a likely candidate, since the E1, 2, and 3 subunits have been shown to interact with the channel (Abbott et al., 1999; McDonald et al., 1997; Schroeder et al., 2000). Currents recorded from cells

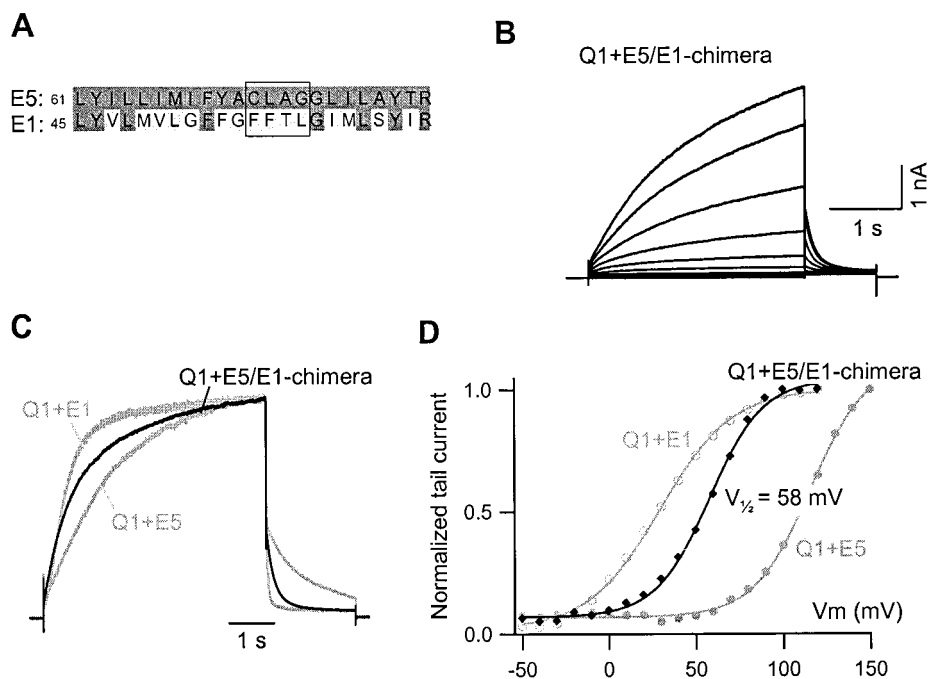


**FIGURE 7** A KCNE5/E1 chimera. (A) Alignment of the transmembrane regions of E1 and E5. The amino acids, which have been substituted in the E5/E1 chimera are boxed. (B) A whole-cell recording from a CHO cell cotransfected with Q1 and the E5/E1 chimera. The cell was clamped according to the protocol in Fig. 1. (C) Superimposed currents of the Q1+E5/E1 chimera (black trace) and the Q1+E5 and Q1+E1 (gray traces). The cells were clamped at +100 mV for 5 s and subsequently at  $-30$  mV for 2 s. Each trace was normalized to the maximal current amplitude measured at the end of the 100-mV pulse. (D) The activation curve of the Q1+E5/E1 chimera (black line). The peak amplitudes of  $-30$ -mV tails from a representative experiment were normalized to the tail current preceded by a 120-mV prepulse. Tail current data were fitted to the Boltzmann function and  $V_{1/2}$  was determined to 58 mV ( $54 \pm 4$  mV,  $n = 5$ ). The activation curves of Q1+E1 and Q1+E5 from Fig. 2 are included for comparison (gray lines).

transfected with hERG1 cDNA alone and in combination with E5 cDNA are presented in Fig. 6 D. The cells were voltage clamped with the same protocol as the KCNQ channels. Our recording revealed no effects of the E5 protein on the hERG1 current.

In the experiments shown in Fig. 6 there is a tendency toward lower current densities in cells expressing the  $\alpha$ -subunit plus E5 as compared to those expressing the  $\alpha$ -subunit alone. Current amplitudes measured at 0 mV were compared and only the current densities of the Q4 channel in the two situations were found to be significantly different ( $p < 0.05$ ); the current density of the Q4  $\alpha$ -subunit was  $213 \pm 57$  pA/pF ( $n = 4$ ) and  $44 \pm 14$  pA/pF for the Q4+E5 ( $n = 5$ ).

### A KCNE5/E1 chimera

Through chimeric studies it has been demonstrated that the amino acids 57, 58, and 59 in the transmembrane domain of E1 are responsible for the E1 control of slow Q1 activation (Melman et al., 2001). Piccini et al. (1999) have aligned the transmembrane region of the E5 and E1 protein sequences and found a homology of 95% (34% identity) (Piccini et al., 1999)(Fig. 7 A). To examine if this particular part of the E5 protein mediates the effect on the activation kinetics of Q1, we made an E5/E1 chimera where the E5 residues 72–75

were substituted with the corresponding E1 residues 56–59 (boxed residues in Fig. 7 A). Fig. 7 B shows a recording of the Q1+E5/E1 chimera where the cell was voltage-clamped at potentials between  $-80$  and  $+100$  mV for 3 s followed by a step to  $-30$  mV for 1 s (same protocol as in Fig. 1). The Q1+E5/E1 chimera exhibited a mixture of E5 and E1 features. In Fig. 7 C the current of the chimera elicited by clamping at +100 mV for 5 s followed by a step to  $-30$  mV for 2 s has been normalized and superimposed on Q1+E1 and Q1+E5 traces. The activation of the Q1+E5/E1 chimera resembled that of Q1+E1. The time constant of activation of the Q1+E5/E1 chimera was determined to  $828 \pm 69$  ms ( $n = 5$ ). This  $\tau_{act}$  value was significantly different from the  $\tau_{act}$  of the Q1+E5 ( $P \ll 0.05$ ) but not significantly different from the  $\tau_{act}$  of the Q1+E1 ( $p > 0.05$ ). As can be seen in Fig. 7 C the tail current of the Q1+E5/E1 chimera mostly resembles that of Q1+E5. The fast and slow constants of deactivation were  $149 \pm 7$  ms and  $2505 \pm 118$  ms ( $n = 5$ ), respectively. The fast component comprised a fraction of  $0.80 \pm 0.04$ . Moreover, the control of voltage sensitivity by the chimera is different from that of E5 subunit. The activation threshold of the Q1+E5/E1 chimera was 0–10 mV and the activation curve in Fig. 7 D shows that the midpoint of activation ( $54 \pm 4$  mV,  $n = 5$ ) was shifted back in the negative direction to a value closer to

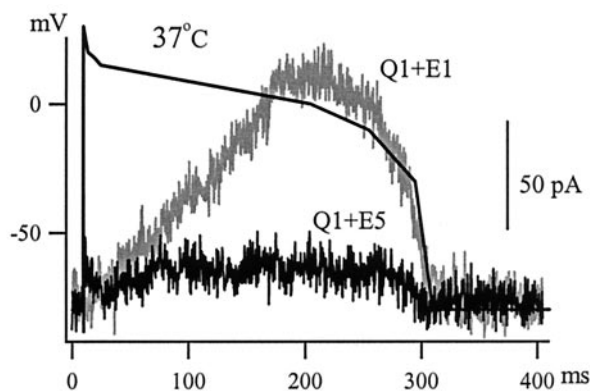


**FIGURE 8** The KCNQ1+KCNE5 current and the cardiac action potential. CHO cells expressing Q1 together with E1 or E5 were stimulated with a voltage protocol modeled on the basis of the human ventricular cardiac action potential (*bold black line*). The holding potential was  $-80$  mV and the protocol peaked at  $+30$  mV and had a duration of 300 ms. The action potential protocol was repeated at a frequency of 2 Hz and all experiments were performed at  $37^{\circ}\text{C}$ . The presented currents are the subtraction product of recordings made before and after block by  $100\ \mu\text{M}$  XE991. The figure shows that the Q1+E1 current rises during the plateau phase of the action potential and peaks at 90 pA after 220 ms ( $66 \pm 18$  pA,  $n = 6$ ). In contrast, only very little Q1+E5 current developed under stimulation with an action potential model ( $17 \pm 7$  pA,  $n = 4$ ).

$V_{1/2}$  of the Q1+E1 ( $p > 0.047$ ) than to the  $V_{1/2}$  of the Q1+E5 complex ( $p < 0.01$ ).

### The KCNQ1+KCNE5 current and the cardiac action potential

The Q1 channel together with the E1 subunit are thought to be the molecular components behind the slowly delayed rectifier current,  $I_{Ks}$ , in the heart (Barhanin et al., 1996; Sanguinetti et al., 1996). Piccini et al. (1999) observed mRNA of E5 in human heart, which lead us to speculate on the functional consequence of E5 expression in cardiac tissue. Fig. 8 shows the response at  $37^{\circ}\text{C}$  to voltage-stimulation with a model of the ventricular action potential when the Q1 channel was expressed in the CHO cells with either the E1 or the E5 subunit. The gray trace in Fig. 8 represents the Q1+E1 current, which rose slowly during the plateau phase and reached a maximum of 90 pA after 220 ms ( $66 \pm 18$  pA,  $n = 6$ ). Clearly, this outward potassium conductance contributes to repolarization. At the end of the 300 ms pulse when the potential dropped back to the holding potential the Q1+E1 current rapidly decreased. The Q1+E5 current is presented by the black trace. Despite the fast activation of the Q1+E5 current at  $37^{\circ}\text{C}$  the right shift in voltage-dependency lead to strong suppression of the Q1 current during execution of the action potential protocol ( $17 \pm 7$  pA,  $n = 4$ ). The average current value was not significantly different from zero.

### DISCUSSION

Association of the Q1 channel with the E5 protein results in significant changes of the kinetics of the Q1 current. Most importantly E5 shifts the voltage activation curve of Q1 by more than 140 mV in the positive direction. Thus, the Q1+E5 channel only activates upon strong and sustained voltage depolarization, meaning that at physiologically relevant potentials the E5 subunit completely suppresses the Q1 current. Despite the changes in gating properties the pore retains potassium selectivity and the current is sensitive to XE991.

The Q1+E5 current activates slowly and deactivates rapidly compared to Q1 alone, albeit with a significant temperature dependency. When the temperature was raised to  $37^{\circ}\text{C}$  the activation time constant and the fast deactivation component of Q1+E5 decreased by fivefold and sixfold, respectively. In comparison the Q1+E1 time constants changed by onefold and threefold, respectively.

By constructing an E5/E1 chimera we found that the amino acids 72–75 of the E5 protein were primarily responsible for the E5 control of the activation and voltage sensitivity of Q1. The activation time and  $V_{1/2}$  of the Q1+E5/E1 chimera were similar to the Q1+E1 current and significantly different from those of the Q1+E5 current. In agreement with Melman et al. (2001), who found that E1 residues responsible for control of deactivation lie outside the 57–59 amino acid segment, the E5/E1 chimera retained most of the E5 effect on the deactivation kinetics of KCNQ1. Thus, similar to E1 there is a physical separation between structural components of the E5 protein that control activation and deactivation.

Piccini et al. (1999) found expression of E5 in human heart by Northern blot analysis and they identified E5 in the heart tissue of mouse embryo with in situ hybridization. Our results showed that in a heterologous expression system E5 strongly suppressed the Q1 current at physiological relevant potentials. A reduction or depletion of the  $I_{Ks}$  current has been proved to be associated with prolonged repolarization of cardiac myocytes (Sanguinetti, 1999). Thus, it could be argued that expression of E5 in the heart would involve a potential danger of acquiring long QT syndrome type 1. It is well known that  $I_{Ks}$  current densities differ between myocardial regions and between species (Nerbonne, 2000). These differences in the  $I_{Ks}$  current and other voltage gated  $\text{K}^+$  currents are responsible for the variations in the action potential waveform of the mammalian heart. Interestingly, the distribution of the Q1 protein has recently been proved to be homogeneously distributed throughout mouse heart (Franco et al., 2001). It could be speculated that the differences in densities of the  $I_{Ks}$  current occur through a differential expression pattern of the E5 subunit (as well as the E1). A corresponding mechanism has been suggested for the transient outward current ( $I_{to}$ ), where reg-

ulation of the KChIP2  $\beta$ -subunit gene expression accounts for the gradient of  $I_{to}$  current through the ventricular wall (Rosati et al., 2001). A  $\beta$ -subunit regulation of the  $I_{Ks}$  current would be a fast and dynamic way of responding to changes in (patho)physiological conditions that involve electrical remodeling.

In this study no effect was found of E5 on the Q2/3, the Q5, or on the hERG1 channel. However, the Q4 current amplitude was found to be significantly suppressed in the presence of E5. It is possible that E5 plays a role in regulating the Q4 expression in sensory hair cells (Kharkovets et al., 2000). AMME patients have diminished hearing sensitivity (Piccini et al., 1999), which could be related to lack of E5 expression and subsequently malfunctioning of  $K^+$  recycling. Whether E5 is expressed in the inner ear has yet to be studied.

Even though the E5 subunit does not change the kinetics of any of the other channels tested except Q1 it can still be speculated that E5 provides the  $\alpha$ -subunits with features such as sensitivity to second messengers, cell volume changes, or pharmacological modulators. Here, these possibilities were not investigated further.

As we learn more about the KCNEs we find that they are promiscuous in their choice of  $\alpha$ -subunit. The KCNE2 and KCNE3 subunits have been found to interact with members of the HCN- and Kv channel families (Yu et al., 2001; Zhang et al., 2001; Abbott et al., 2001). Perhaps the Q1 channel is not the only partner of the E5  $\beta$ -subunit. Apart from the heart, mRNA of E5 was also observed in human skeletal muscle, brain, spinal cord and placenta (Piccini et al., 1999); E5 may serve as a  $\beta$ -subunit of other channels in these tissues.

Our observations question that E1 should be the only  $\beta$ -subunit regulating the  $I_{Ks}$  current in the heart. We suggest that the E5 could account for the variations of the  $I_{Ks}$  current density in the heart. Whether the E5 protein couples to the Q1 channel in vivo will be investigated through localization studies and immunoprecipitation from native heart tissue when E5 specific antibodies become available.

We thank Inge Kjeldsen and Pia Hageman for technical assistance. This study was supported by the Danish Heart Association.

## REFERENCES

Abbott, G. W., M. H. Butler, S. Bendahhou, M. C. Dalakas, L. J. Ptacek, and S. A. Goldstein. 2001. MiRP2 forms potassium channels in skeletal muscle with Kv3.4 and is associated with periodic paralysis. *Cell*. 104:217–231.

Abbott, G. W., F. Sesti, I. Splawski, M. E. Buck, M. H. Lehmann, K. W. Timothy, M. T. Keating, and S. A. Goldstein. 1999. MiRP1 forms IKr potassium channels with HERG and is associated with cardiac arrhythmia. *Cell*. 97:175–187.

Barhanin, J., F. Lesage, E. Guillemare, M. Fink, M. Lazdunski, and G. Romey. 1996. K(V)LQT1 and IsK (minK) proteins associate to form the I(Ks) cardiac potassium current. *Nature*. 384:78–80.

Baud, C., R. T. Kado, and K. Marcher. 1982. Sodium channels induced by depolarization of the *Xenopus laevis* oocyte. *Proc. Natl. Acad. Sci. U.S.A.* 79:3188–3192.

Franco, D., S. Demolombe, S. Kupersmidt, R. Dumaine, J. N. Dominguez, D. Roden, C. Antzelevitch, D. Escande, and A. F. Moorman. 2001. Divergent expression of delayed rectifier K(+) channel subunits during mouse heart development. *Cardiovasc. Res.* 52:65–75.

Grahammer, F., R. Warth, J. Barhanin, M. Bleich, and M. J. Hug. 2001. The small conductance K+ channel, KCNQ1: expression, function, and subunit composition in murine trachea. *J. Biol. Chem.* 276:42268–42275.

Grunnet, M., B. S. Jensen, S. P. Olesen, and D. A. Klaerke. 2001. Apamin interacts with all subtypes of cloned small-conductance Ca2+-activated K+ channels. *Pflugers Arch.* 441:544–550.

Jespersen, T., M. Grunnet, K. Angelo, D. Klaerke, and S. Olesen. 2002. Dual-function vector for protein expression in both mammalian cells and *Xenopus laevis* Oocytes. *Biotechniques*. 32:536–540.

Jonsson, J. J., A. Renieri, P. G. Gallagher, C. E. Kashtan, E. M. Cherniske, M. Bruttini, M. Piccini, F. Vitelli, A. Ballabio, and B. R. Pober. 1998. Alport syndrome, mental retardation, midface hypoplasia, and elliptocytosis: a new X linked contiguous gene deletion syndrome? *J. Med. Genet.* 35:273–278.

Kharkovets, T., J. P. Hardelin, S. Safieddine, M. Schweizer, A. El Amraoui, C. Petit, and T. J. Jentsch. 2000. KCNQ4, a K+ channel mutated in a form of dominant deafness, is expressed in the inner ear and the central auditory pathway. *Proc. Natl. Acad. Sci. U.S.A.* 97:4333–4338.

McDonald, T. V., Z. Yu, Z. Ming, E. Palma, M. B. Meyers, K. W. Wang, S. A. Goldstein, and G. I. Fishman. 1997. A minK-HERG complex regulates the cardiac potassium current I(Kr). *Nature*. 388:289–292.

Melman, Y. F., A. Domenech, L. S. de la, and T. V. McDonald. 2001. Structural determinants of KvLQT1 control by the KCNE family of proteins. *J. Biol. Chem.* 276:6439–6444.

Nerbonne, J. M. 2000. Molecular basis of functional voltage-gated K+ channel diversity in the mammalian myocardium. *J. Physiol.* 525 Pt 2:285–298.

Peleg, S., D. Varon, T. Ivanina, C. W. Dessauer, and N. Dascal. 2002. G $\alpha$ (i) controls the gating of the G protein-activated K(+) channel, GIRK. *Neuron*. 33:87–99.

Piccini, M., F. Vitelli, M. Seri, L. J. Galletta, O. Moran, A. Bulfone, S. Banfi, B. Pober, and A. Renieri. 1999. KCNE1-like gene is deleted in AMME contiguous gene syndrome: identification and characterization of the human and mouse homologs. *Genomics*. 60:251–257.

Robbins, J. 2001. KCNQ potassium channels: physiology, pathophysiology, and pharmacology. *Pharmacol. Ther.* 90:1–19.

Rosati, B., Z. Pan, S. Lypen, H. S. Wang, I. Cohen, J. E. Dixon, and D. McKinnon. 2001. Regulation of KChIP2 potassium channel beta subunit gene expression underlies the gradient of transient outward current in canine and human ventricle. *J. Physiol.* 533:119–125.

Sanguinetti, M. C. 1999. Dysfunction of delayed rectifier potassium channels in an inherited cardiac arrhythmia. *Ann. N. Y. Acad. Sci.* 868:406–413.

Sanguinetti, M. C., M. E. Curran, A. Zou, J. Shen, P. S. Spector, D. L. Atkinson, and M. T. Keating. 1996. Coassembly of K(V)LQT1 and minK (IsK) proteins to form cardiac I(Ks) potassium channel. *Nature*. 384:80–83.

Schroeder, B. C., S. Waldegger, S. Fehr, M. Bleich, R. Warth, R. Greger, and T. J. Jentsch. 2000. A constitutively open potassium channel formed by KCNQ1 and KCNE3. *Nature*. 403:196–199.

Seino, S. 1999. ATP-sensitive potassium channels: a model of heteromultimeric potassium channel/receptor assemblies. *Annu. Rev. Physiol.* 61:337–362.

Sesti, F. and S. A. Goldstein. 1998. Single-channel characteristics of wild-type IKs channels and channels formed with two minK mutants that cause long QT syndrome. *J. Gen. Physiol.* 112:651–663.

Sigworth, F. J., H. Afolter, and E. Neher. 1995. Design of the EPC-9, a computer-controlled patch-clamp amplifier. 2. Software. *J. Neurosci. Methods*. 56:203–215.

- Strobaek, D., T. D. Jorgensen, P. Christophersen, P. K. Ahring, and S. P. Olesen. 2000. Pharmacological characterization of small-conductance Ca(2+)-activated K(+) channels stably expressed in HEK 293 cells. *Br. J. Pharmacol.* 129:991–999.
- Takumi, T., H. Ohkubo, and S. Nakanishi. 1988. Cloning of a membrane protein that induces a slow voltage-gated potassium current. *Science*. 242:1042–1045.
- Tinel, N., S. Diochot, M. Borsotto, M. Lazdunski, and J. Barhanin. 2000a. KCNE2 confers background current characteristics to the cardiac KCNQ1 potassium channel. *EMBO J.* 19:6326–6330.
- Tinel, N., S. Diochot, I. Lauritzen, J. Barhanin, M. Lazdunski, and M. Borsotto. 2000b. M-type KCNQ2-KCNQ3 potassium channels are modulated by the KCNE2 subunit. *FEBS Lett.* 480:137–141.
- Yu, H., J. Wu, I. Potapova, R. T. Wymore, B. Holmes, J. Zuckerman, Z. Pan, H. Wang, W. Shi, R. B. Robinson, M. R. El Maghrabi, W. Benjamin, J. Dixon, D. McKinnon, I. S. Cohen, and R. Wymore. 2001. MinK-related peptide 1: A beta subunit for the HCN ion channel subunit family enhances expression and speeds activation. *Circ. Res.* 88:E84–E87.
- Zhang, M., M. Jiang, and G. N. Tseng. 2001. minK-related peptide 1 associates with Kv4.2 and modulates its gating function: potential role as beta subunit of cardiac transient outward channel? *Circ. Res.* 88:1012–1019.